Synthesis and Characterization of Silver/Zein Nanocomposites and Their Application

Omayma A. Ghazy,[1] Shimaa Nabih,[2] Yasser K. Abdel-Moneam,[3] Magdy M. Senna[1]
[1]*Radiation Chemistry Department, National Center for Radiation Research and Technology, Nasr City, Cairo, Egypt*

[2]*Basic Science Department, Modern Academy for Engineering and Technology, Madi, Egypt*

[3]*Faculty of Science Chemistry Department, Menoufia University, Shibin El Kom, Egypt*

Zein nanoparticles were prepared by the liquid-liquid dispersion method. The particles were used as templates for growing silver nanoparticles by reduction of silver ions using gamma radiation. The dynamic light scattering and transmission electron microscopy (TEM) results indicated that the obtained zein nanoparticles have spherical shape with a homogeneous particle size distribution and an average particle size of 60 nm. The factors affecting the silver nanoparticle deposition on zein nanoparticles were studied. Among these factors, irradiation dose, silver ion concentration, and zein polymer content were evaluated. The formation of the nanocomposite was detected using UV–vis spectroscopy and TEM. The surface plasmon resonance peak was found to be sensitive to the concentration of the zein and $AgNO_3$ solutions. A blue shift was observed as the zein content was increased, while a red shift took place upon increasing the $AgNO_3$ concentration. The TEM imaging indicated that the silver particles are nanosized, spherical in shape and adsorbed on the surface of zein particles. The Zein/silver nancomposites were applied for the antimicrobial test against *E. coli* and found to have high antibacterial activity. POLYM. COMPOS., 38:E9–E15, 2017. © 2015 Society of Plastics Engineers

INTRODUCTION

Metal nanoparticles incorporated in polymer matrices are gaining more attention because polymers prevent their agglomeration and help for their recovery upon usage. The function can be even complementary between the polymer and the metal nanoparticles [1]. Silver nanoparticles, has been extensively studied in several applications such as catalysis, surface enhanced Raman spectroscopy (SERS) and biomedical applications [2–12]. Biopolymers have been gaining more interest in wide scope of applications due to their nontoxicity and biocompatibility. Zein is the maize protein, its structure contains a large number of hydrophobic amino acids. Micro and nanospheres based on zein have been used for different applications, including encapsulation of food stuffs [13], encapsulation of vitamin D3 [14] drug delivery systems [15–17], and biomineralization [18]. Zein structure is very attractive for the interaction with metal ions, where the amine and hydroxyl groups can form coordination bonds with them. The control of the metal particle size is important for its function, the antimicrobial activity of silver nanoparticles was found to alter with the particle shape and size [19, 20]. The balance between the nucleation rate and the particle growth controls the particles size and shapes; this is believed to be highly affected by the method of reduction. The preparation of metal nanoparticles is done by the mild chemical reduction for metal salt solutions. Other methods such as the radiochemical and photochemical reduction are also common [21]. In the radiochemical method, the solvated electrons generated by water hydrolysis can reduce metal ions [22, 23]. This method has the advantage of producing metal nuclei homogenously and instantaneously. Moreover, the particles have narrow particle size distribution. In addition, the nanoparticles produced in such methods do not need excessive steps of purification due to the lack of contaminants. Recently, composites of zein solutions and silver nanoparticles were prepared [24, 25]. However the presence of ethanol as a solvent for zein may limit the applications of the composite. Dispersing zein in water makes it suitable for more applications such as self-care products and medical applications. In this work, zein nanoparticles were prepared by the liquid-liquid dispersion method. Silver/zein Nanocomposites were prepared by gamma radiation induced reduction of silver ions on the surface of zein nanoparticles.

Correspondence to: O.A. Ghazy; e-mail: omayma_gh@yahoo.com
DOI 10.1002/pc.23791
Published online in Wiley Online Library (wileyonlinelibrary.com).

The effect of $AgNO_3$ and zein concentrations was investigated and the properties of the produced nanoparticles were characterized in terms of Dynamic light scattering (DLS), UV–visible spectroscopy, and TEM. The nancomposites were applied for the antimicrobial test against *E. coli*.

EXPERIMENTAL

Material

Silver nitrate, zein, and ethanol were obtained from (Sigma-Aldrich, Canada; Oakville, ON, Canada). All chemicals were of analytical grade and used without further purification. All aqueous solutions were made using deionized water.

Preparation of Zein Nanoparticles

The zein nanoparticles were prepared according to the liquid-liquid dispersion method described earlier in the literature [26, 27]. The required weight of zein was dissolved in ethanol/H_2O (4:1) mixture. After that, zein solution was added to distilled water, ethanol was then evaporated, and the zein nanoparticles were obtained as nanodispersion.

Preparation of Ag/Zein Nanocomposites

Different samples (Table 1) were prepared by adding different concentrations of $AgNO_3$ to different zein nanodispersions under constant stirring. The $AgNO_3$/zein solutions were irradiated with Co-60 gamma source at different doses.

Gamma Irradiation

The direct radiation technique was used, in which $AgNO_3$/zein solutions were exposed to gamma radiation at various irradiation doses. The dose rate was determined using a Fricke dosimeter and was found to be 2.86 kGy/h for the self-shielded Indian gamma cell facility installed at the National Center for Radiation Research and Technology, Cairo, Egypt.

UV–Vis Spectroscopic Analysis

UV/vis analysis was carried out using a UV2 double beam Unicam, England over the range 200–800 nm at a high resolution scans.

Transmission Electron Microscopy (TEM)

The morphology of the particles was investigated using TEM images model JEM 100CS, Jeol, Japan, working at acceleration voltage of 80 kV.

TABLE 1. Sample coding based on $AgNO_3$/zein compositions.

Sample no.	Zein/solvent wt/v (%)	Concentration of $AgNO_3$ (M)
M1	0.50	—
M2	0.33	0.010
M3	0.67	0.010
M4	0.83	0.010
M5	0.50	0.004
M6	0.50	0.007
M7	0.50	0.014
M8	0.50	0.040

Dynamic Light Scattering

The particle size distribution of zein nanoparticles was determined using the Nicomp 380ZLS, PSSNICOMP, particle sizing system, Santa Barbara.

Antibacterial Activity

The antibacterial activity of the zein/silver nanocomposites against *Escherichia coli* was evaluated by observing the suppression of *E. coli* growth and measuring the inhibition zone for samples incubated at 37°C. The discs were placed on a surface of nutrient agar (HiMedia Laboratories, India), which had been previously seeded with 20 μL of inoculum containing tested bacteria, that is, *E. coli*. The plates were incubated at 37°C for 24 h, the contact areas of the composite with agar surface were observed. The inhibitory efficiency related to the size of the inhibition zone, that is, the larger the clear area around the film, the higher the inhibitory efficiency.

RESULTS AND DISCUSSION

Preparation and Characterization of Zein Nanoparticles

Figure 1 shows the TEM image of zein nanoparticles (M1) and the associated particle size histogram. The particles are shown to be spherical in shape with an average particle size of 60 nm. However these nanoparticles are connected to each other this. Finding was also observed by others [14], who used a low energy method for the homogenization of zein solution in water, as in our case. In contrary to other studies that used high share homogenizers for the homogenization process, they obtained individual zein nanoparticles [28, 29]. The particle size distribution of zein nanoparticles as measured by DLS is shown in Fig. 2. The mean particle size is 250 nm, which is larger than that observed by TEM. The difference is most probably due to the presence of interconnections between the nanoparticles. The polydispersity index PDI measured by DLS reflects the particle size distribution. In our case, it is 0.23, a small value indicating a uniform particle size. The structure of zein contains polar regions

 DOI 10.1002/pc

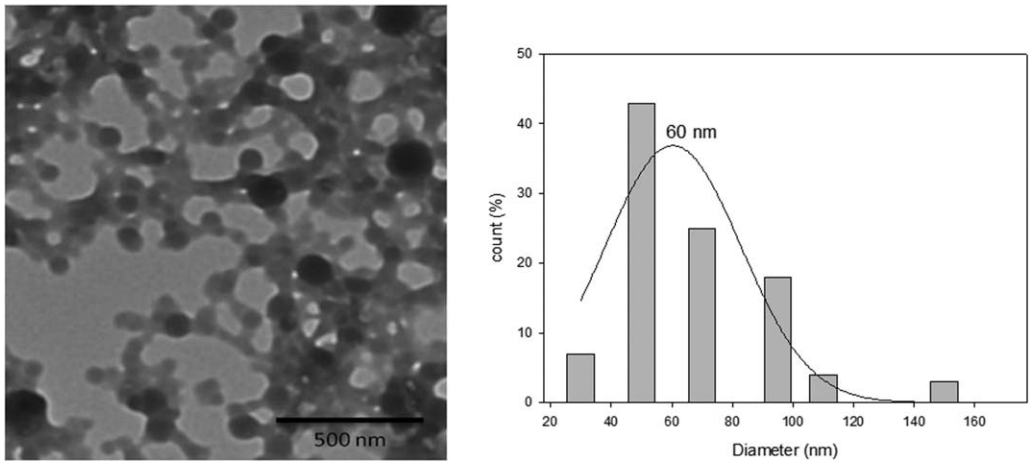

FIG. 1. TEM image of zein nanoparticles and the associated particle size histogram.

and nonpolar regions [30]. The polar regions contain functional groups such as amino, carboxylic, and hydroxyl groups. During the particle formation, these regions are assumed to orient themselves on the surface of the particles with the functional groups facing the aqueous phase, as illustrated in Fig. 3. Such orientation should be preferable for the particles, since the interaction of the polar' regions with the aqueous phase decreases the interfacial tension between the two phases and the particles acquire minimum surface energy.

Preparation of Silver/Zein Nanocomposite

The functional groups on the surface of zein nanoparticles, mainly NH_2, COOH, and OH, have the affinity to coordinatet with metal ions. This advantage was used to grow silver nanoparticles on the surface of zein nanoparticles. For all samples, the silver ions were incubated for 24 h with the latex particles in order to give enough time for the silver ions to coordinate with the functional groups on the surface of the latex. After that, gamma irradiation was used for the reduction of silver ions on the surface of zein particles. The first observation for all the reduced samples is that the color was turned to brown color and no silver mirror was observed on the glassware, which means that all the formed silver nanoparticles are adsorbed on the surface of the zein nanoparticles.

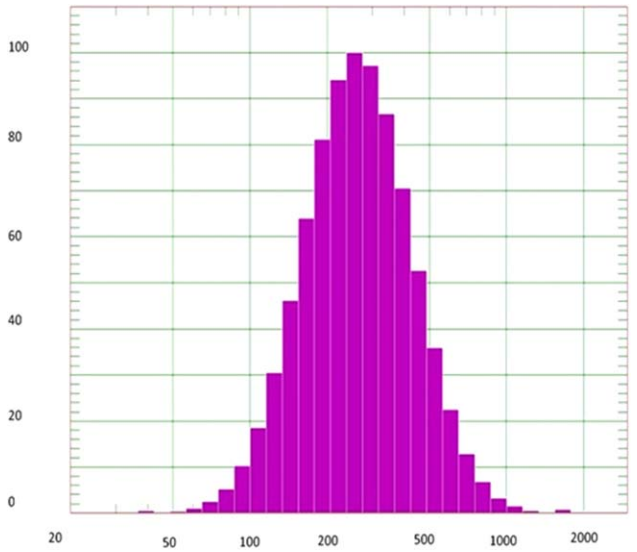

FIG. 2. Particle size distribution of zein nanoparticles, as measured by DLS.

UV–Vis Analysis

Silver nanoparticles are known to exhibit an intense surface plasmon absorption band in the range of (400–500 nm) according to the particle size, and the local refractive index near the particle surface [31, 32]. The effect of the gamma ray doses as well as the concentration of silver ions and zein on the formation of the surface plasmon resonance bands are presented here.

Effect of Irradiation Dose

The effect of irradiation dose (1–10 kGy) on the formation of the surface plasmon resonance bands of silver nanoparticles for the sample prepared using 0.007 M

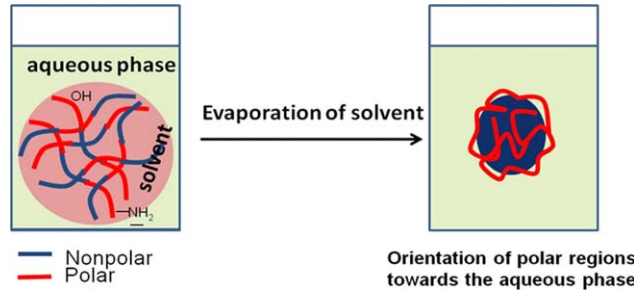

FIG. 3. Orientation of polar regions toward the aqueous phase, during the particles formations.

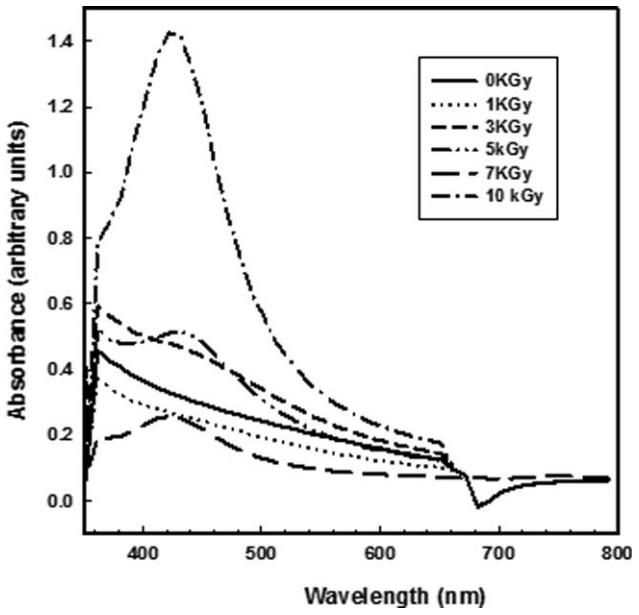

FIG. 4. UV–vis spectra of silver/zein nanocomposite (M6) prepared by different doses of gamma radiation.

silver ions and 0.5% wt/v of zein dispersion (M6) is shown in Fig. 4.

It can be seen that the band corresponding to the silver surface plasmon at 420 nm started to appear at irradiation dose of 5 kGy, before which no band was detected. The band became very sharp at 10 kGy. This result is in a good agreement with Long et al. [33] who revealed that silver nanoparticles could not be formed at gamma-ray dose less than 5 kGy, and no more difference were found for higher doses. During the radiolysis, a large number of homogenously distributed hydrated radicals are produced. The hydrated electrons are capable of reducing all the silver ions to silver atoms. These atoms act as nuclei for the successively formed atoms. The process is illustrated in Scheme 1.

Effect of Zein Concentration

The content of zein was varied from 0.33 to 0.83 wt/v% (M2-M4) with a constant concentration of Ag ions (0.01 M) and irradiated at 10 kGy. The UV spectra of the irradiated

$$H_2O \xrightarrow{GammaRays} e^-_{aq} + H_3O^+ + H^0 + H_2 + OH^0 + H_2O_2 + ...$$

$$Ag^+ + e^-_{aq} \xrightarrow{\text{Reduction}} Ag^0$$

$$Ag^0 + Ag^+ \rightarrow Ag^+_2$$

$$Ag^0 + Ag^+_2 \rightarrow Ag^+_3$$

$$(Ag)^+_n + e^-_{aq} \rightarrow (Ag)_n$$

SCH. 1. Reduction of silver ions by the hydrated electrons produced during radiolysis.

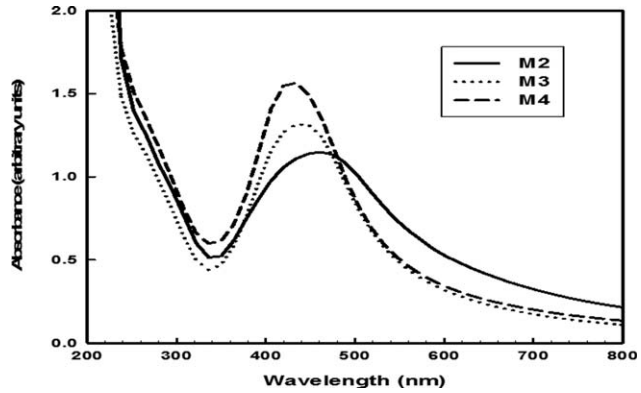

FIG. 5. UV–vis spectra of silver/zein nanocomposites prepared by constant $AgNO_3$ concentration (0.01M) and different zien concentrations: M2 (0.33), M3 (0.67), and M4 (0.83) wt/v%.

samples were shown in Fig. 5. From the figure, it can be seen that the plasmon resonance peaks were shifted from 458 to 428 nm with increasing the zein content from 0.33 to 0.83 wt/v%. This blue shift indicates the formation of smaller particles [34]. In addition, the intensity of the plasmon resonance peaks was increased with increasing zein content. This effect may be due to the availability of more functional groups to coordinate with silver ions, which means more nuclei are formed upon reduction resulting in the formation of more particles with smaller size.

Effect of Silver Ion Concentration

Different concentrations of silver ions were used namely, 0.004, 0.007, 0.014, and 0.04 M (M5-M8). A constant content of zein was used (0.5 wt/v%). The samples were gamma irradiated at 10 kGy. The UV–visible spectra

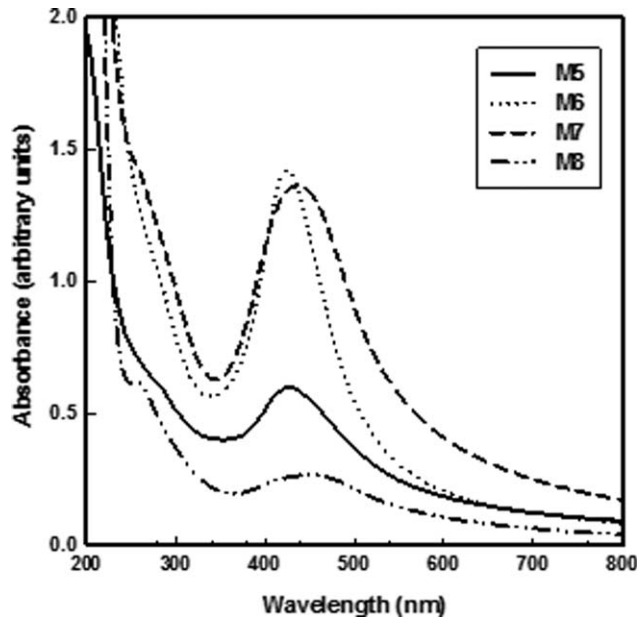

FIG. 6. UV–vis spectra of silver/zein nanocomposites prepared by constant zein concentration (0.5 wt/v%) and different $AgNO_3$ concentrations: M5 (0.004), M6 (0.007), M7 (0.014), and M8 (0.04) M.

DOI 10.1002/pc

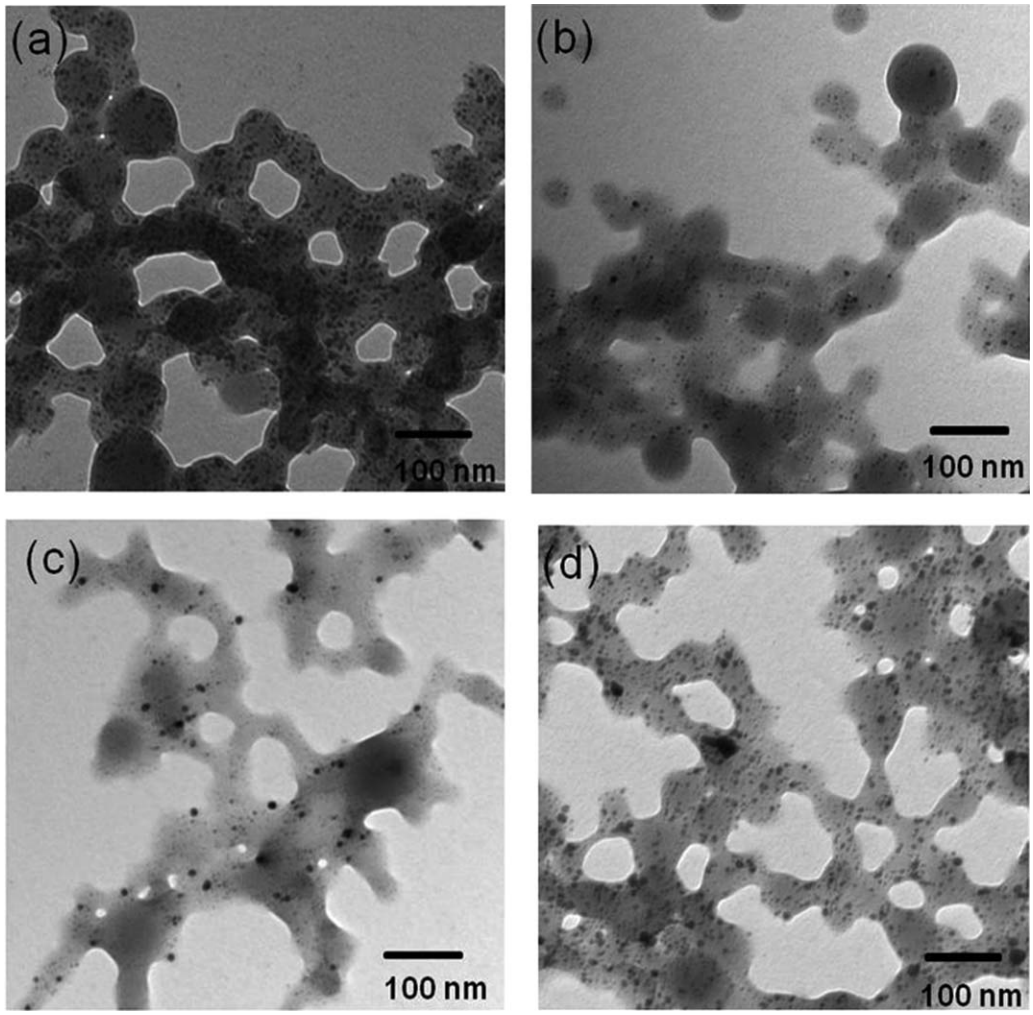

FIG. 7. TEM images of silver/zein nanocomposites: (a) M2, (b) M4, (c) M5, and (d) M6.

of the samples show increment of the intensity of the surface palsmon with increasing the concentration of the silver ions (Fig. 6). A red shift is also observed for the samples prepared with higher silver ion concentrations. This observation suggests the formation of larger silver nanoparticles. As a general observation, all the UV–visible spectra show symmetric and nonsplitting bands; this indicates that the silver nanoparticles are homogeneous spherical particles [35, 36]. This will be further confirmed by the TEM results.

TEM Analysis

Figure 7a–d shows the TEM images of different silver stabilized zein nanoparticles. The images indicate that all the formed silver nanoparticles are adsorbed on the surface of zein nanoparticles and no separate Ag clusters were formed. As can be seen in the figure, the silver nanoparticles have spherical shape and no other shapes were observed. This result is agreeing well with the results of the UV–visible spectroscopy. Two samples were prepared with the same concentration of silver ions (0.01 M) and different zein contents 0.33% (M2) and 0.83% (M4) and irradiated with the same radiation dose (10 kGy). Figure 7a and b shows the TEM of the M2 and M4, respectively. It is noticeable that the silver nanoparticles formed in M2 are more than those formed in M4. The silver nanoparticles in M4 are also finer in size. The samples prepared with the same zein content (0.5%) and different silver nitrate content; M5 (0.004 M) and M6 (0.007 M) are shown in Fig. 7c and d, respectively. The two samples were exposed to 10 kGy irradiation dose. The density of the formed silver nanoparticles in M6 is pronouncedly higher as shown in the figure. The results indicate that as the amount of the functional groups of zein increases in relation to the concentration of the silver ions, more nuclei are formed upon reduction. This results in the formation of finer silver nanoparticles. In this concern, zein is not only working as stabilizer for silver nanoparticles but also as size controller by adjusting its relative concentrations with silver ions.

Antimicrobial Activity of Zein/Silver Nanocomposites

The antimicrobial activity of zein/silver nanocomposites against *E. coli* that was applied as model Gram-

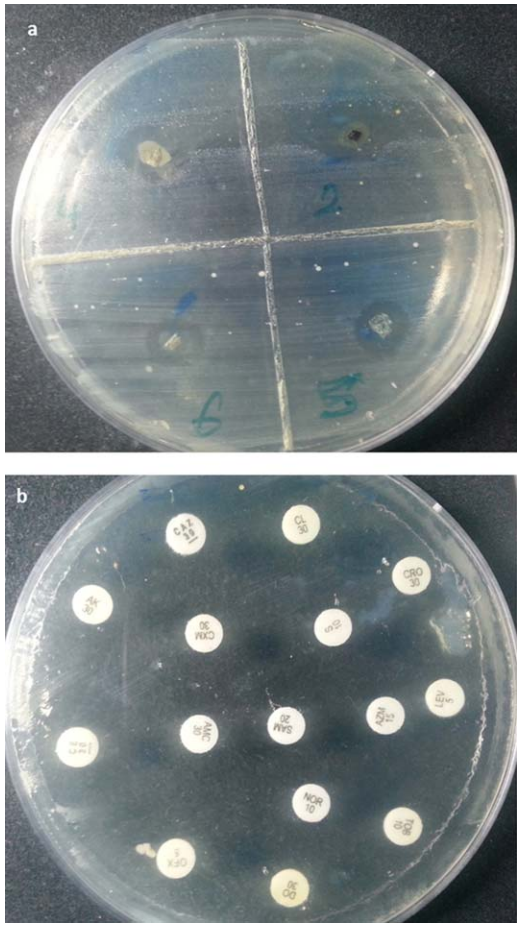

FIG. 8. Photographs of antimicrobial test results against *E. coli* (a) zein/silver nanocomposite and (b) standardantimicrobial discs.

negative bacteria was studied by an agar diffusion method. After 24 h incubation at 37°C, the contact areas of all zein/silver nanocomposites with agar surface turned transparent indicating the inhibition of bacteria growth (Fig. 8a). However, clear zones surrounding the standard discs were observed only for Ame, Sam, CE, and Ak, on the other hand S, DO, and Nor were less effective (Fig. 8b). This implies that zein/silver nanocomposites exhibited inhibitory activity against *E. coli*. The antibacterial activity of zein/silver nanocomposites may due to the adherence of silver nanoparticles to the surface of the bacteria cell membrane and consequently disturbed its respiration via interacting with enzymes of respiratory chains [37]. This result indicates that zein/silver nanocomposites have an excellent biocidal effect and potential in reducing bacterial growth for practical applications.

CONCLUSIONS

Stable zein nanoparticles with an average particle size of 60 nm were prepared by the liquid –liquid dispersion method. Zein/silver nanocomposites were prepared by gamma radiation induced reduction of silver ions on the surface of zein nanoparticles. The UV–visible spectroscopy and TEM measurements confirmed that the size and plasmonic properties of silver nanoparticles could be tuned by controlling the relative concentrations of zein polymer and silver ions. Where, smaller silver nanoparticles were obtained by increasing the zein polymer content while larger particles were obtained by increasing the silver ion concentration. The zein/silver nanocomposites were found to have antibacterial activity against *E. coli*. The novel composite material can find wide range of applications in the biomedical field.

ACKNOWLEDGMENT

The authors would like to thank Prof. Dr. Monique Lacroix, INRS-Institut Armand-Frappier, Canadian Irradiation Centre, Research Laboratories in Sciences Applied to Food, for her comments and suggestions.

REFERENCES

1. L.E. Stron and J.L. West, *Nanomed. Nanobiotechnol.*, **3**, 307 (2011).
2. J.Z. Guo, H. Cui, W. Zhou, and W. Wang, *Photochem. Photobiol. Chem.*, **193**, 89 (2008).
3. A. Mayer, W. Grebner, and R. Wannemacher, *J. Phys. Chem. B*, **104**, 7278 (2000).
4. G. Braun, I. Pavel, A.R. Morrill, D.S. Seferos, G.C. Bazan, N.O. Reich, and M. Moskovits, *J. Am. Chem. Soc.*, **129**, 7760 (2007).
5. T. Shegai, Z. Li, T. Dadosh, Z. Zhang, H.X. Xu, and G. Haran, *Proc. Natl. Acad. Sci. USA*, **105**, 16448 (2008).
6. J.S. Kim, E. Kuk, K.N. Yu, J.H. Kim, S.J. Park, H.J. Lee, S.H. Kim, Y.K. Park, Y.H. Park, C.Y. Hwang, Y.K. Kim, Y.S. Lee, D.H. Jeong, and M.H. Cho, *Nanomed. Nanotechnol. Biol. Med.*, **3**, 95 (2007).
7. M. Raffi, F. Hussain, T. Bhatti, J.I. Makhter, A. Hameed, and M.M. Hasan, *J. Mater. Sci. Technol.*, **24**, 192 (2008).
8. A. Jing, W. Desong, L. Qingzhi, Y. Xiaoyan, *Mater. Sci. Eng. C*, **29**, 1984 (2009).
9. S. Schultz, D.R. Smith, J.J. Mock, and D. Schultz, *Proc. Natl. Acad Sci. USA*, **97**, 996 (2000).
10. Y.W. Cao, R. Jin, and C.A. Mirkin, *J. Am. Chem. Soc.*, **123**, 7961 (2001).
11. G.N.R. Tripathi, *J. Am. Chem. Soc.*, **125**, 1178 (2003).
12. M. Darroudi, M.B. Ahmad, A.K. Zak, R. Zamiri, and M. Hakimi, *Int. J. Mol. Sci.*, **12**, 6346 (2001).
13. J. Gomez-Estaca, M.P. Balaguer., R. Gavara, and P. Hernandez-Munoz, *Food Hydrocolloids*, **28**, 82 (2012).
14. Y. Luo, Z. Teng, and Q. Wang, *J. Agric. Food Chem.*, **60**, 836 (2012).
15. P. Satheesh and O. Perumal, *J. Biomed. Nanotechnol.*, **6**, 312 (2010).
16. L.F. Lai and H.X. Guo, *Int. J. Pharm.*, **404**, 317 (2011).
17. R.G. Aswathy, B. Sivakumar, D. Brahatheeswaran, T. Fukuda, Y. Yoshida, T. Maekawa, and D.S. Kumar, *Adv. Nat. Sci. Nanosci. Nanotechnol.*, **3**, 1 (2012).

 DOI 10.1002/pc

18. Y. Li and C. Yao, *Polym. Compos.*, **33**, 961 (2012).
19. Y. Jeong, D.W. Lim, and J. Choi, *Adv. Mater. Sci. Eng.*, **2014**, 6 (2014).
20. S. Pal, Y.K. Tak, and J.M. Song, *Appl. Environ. Microbiol.*, **73**, 1712 (2007).
21. R. Yoksan and S. Chirachanchai, *Mater. Chem. Phys.*, **115**, 296 (2009).
22. A. Abedini, F. Larki, E. Saion, A. Zakaria, and M.Z. Hussein, *Radiat. Phys. Chem.*, **81**, 1653 (2012).
23. M. Mostafavi, G.R. Dey, L. François, and J. Belloni, *J. Phys. Chem. A*, 10, 10184 (2002).
24. B. Zhang, Y. Luo, and Q. Wang, *Biomacromolecules*, **11**, 2366 (2010).
25. O.A. Ghazy, Y.K. Abdel-Monem, S. Nabih, and M.M. Senna, *Indian J. Appl. Res.*, **3**, 68 (2013).
26. Y. Dong and S. Feng, *Biomaterial*, **25**, 2843 (2004).
27. T. Higuchi, H. Yabu, and M. Shimomura, *Colloids Surf. A*, **284**, 250 (2006).
28. Q. Zhong and J. Minfeng, *J. Food Hydrocolloid*, **23**, 2380 (2009).
29. N. Parris, P.H. Cooke, and K.B. Hicks, *J. Agric. Food Chem*, **53**, 4788 (2005).
30. E. Corradini, L.H.C. Mattoso, C.G.F. Guedes, and D.S. Rosa, *Polym. Adv. Technol.*, **15**, 340 (2004).
31. K. Esumi and K. K. Torigoe, *Prog. Colloid Polym. Sci.*, **117**, 80 (2002).
32. C. Petit, P. Lixon, and M.P. Pileni, *J. Phys. Chem.*, **97**, 12974 (1993).
33. D. Long, G. Wu, and S. Chen, *Rad. Phys. Chem.*, **76**, 1126 (2007).
34. S.L. Smitha, K.M. Nissamudeen, D. Philip, and K.G. Gopchandran, *Spectrochim. Acta A*, **71**, 186 (2008).
35. A.B.R. Mayer and J.E. Mark, *Polymer*, **41**, 1627 (2000).
36. S.M. Sibdas and K. Niranjan, *Mater. Chem. Phys.*, **112**, 1114 (2008).
37. B.K. Holt and A.J. Bard, *Biochemistry*, **44**, 13214 (2005).